ChemComm

COMMUNICATION

View Article Online
View Journal

Cite this: DOI: 10.1039/d5cc03601a

Received 27th June 2025,
Accepted 31st July 2025

DOI: 10.1039/d5cc03601a

rsc.li/chemcomm

Chemical tuning of a double double perovskite oxide

Azizah Almadhi,[a] Sean D. Injac,[a] Kunlang Ji,[a] Clemens Ritter[b] and J. Paul Attfield *[a]

The feasibility of chemical doping of a double double perovskite (DDPv) is demonstrated by $La_xCa_{1-x}MnMnReO_6$ solid solutions in which cation-site ordering is preserved to $x \geq 0.5$ while La^{3+}/Ca^{2+} substitution at one site tunes magnetic properties. Each of the ~20 DDPv's discovered by high pressure synthesis in recent years is thus a starting point for chemical tuning to discover and tune electronic and magnetic properties.

Perovskite oxides ABO_3 and related materials have a wide range of important physical and chemical properties. An important mechanism for tuning properties is through aliovalent cation substitution, typically compensated by changes in oxidation state of other metals. This is a well-known way to dope ternary oxides, *e.g.* tuning of CMR (colossal magnetoresistance) and associated effects in $La_{1-x}Ca_xMnO_3$ and related manganite perovskites, and of superconductivity in $La_{2-x}Sr_xCuO_4$ and other layered-perovskite cuprates. More complex materials where multiple cation orders are present are also important for electronic or catalytic properties,[1] but chemical doping may induce disorder that disrupts properties of interest. For example, replacing Sr^{2+} by La^{3+} in the ferrimagnetic CMR double perovskite Sr_2FeMoO_6 leads to inversion disorder of the B-site Fe/Mo cations accompanied by a decrease in magnetisation.[2]

As well as leading to $AA'B_2O_6$ or $A_2BB'O_6$ double perovskites (*e.g.* Sr_2FeMoO_6 above),[3,4] 1 : 1 cation ordering in perovskites can lead to $AA'BB'O_6$ double double perovskites (DDPv's) with cation ordering at both sites. Over the last decade, an extensive DDPv family based on columnar A/A′ and rocksalt B/B′ cation orders has been discovered.[5] These materials have a tetragonal (space group $P4_2/n$) perovskite superstructure and are prepared under high pressure (~10 GPa) and high temperature (HPHT) conditions to stabilise order of large A = rare earth R^{3+} or Ca^{2+} and small A′ = transition metal (usually Mn^{2+}) cations. Examples include $RMnMnB'O_6$ for B′ = Sb and Ta,[6,7] $CaMnBReO_6$ (B = Fe, Mn, Co, Ni),[8–10] $CaCuFeReO_6$,[11] and $CaFeFeNbO_6$.[12] This DDPv structure has five distinct cation sites, four of which can be occupied by magnetic transition metal cations (two A′ column sites as well as B and B′ sites) leading to a variety of magnetic properties, including high temperature (~500 K) ferrimagnetism and magnetoresistance in $CaA'FeReO_6$ (A′ = Mn and Cu) DDPvs.[11,13] However, A-site disorder is also observed when some $AA'BB'O_6$ compositions are synthesised at HPHT conditions, written as $(A_{0.5}A'_{0.5})_2BB'O_6$ to emphasise that these are double perovskites with B/B′ cation ordering but without A/A′ order. $(R_{0.5}Mn_{0.5})_2MnB'O_6$ (B′ = Sb and Ta) double perovskites were obtained for small rare earth cations, and both double double and double perovskite polymorphs have been recovered for some compositions, *e.g.* $CaMnMnWO_6$ and $(Ca_{0.5}Mn_{0.5})_2MnWO_6$ from varying temperatures at 10 GPa pressure.[14]

Continuous tuning of properties through aliovalent substitutions has not been reported for any DDPv. To demonstrate that such doping control is possible, and without loss of A/A′ or B/B′ cation orders, we have investigated La^{3+} doping of $CaMnMnReO_6$. This DDPv with charge configuration $Ca^{2+}Mn^{2+}Mn^{2+}Re^{6+}O_6$ was reported to have a high degree of cation order (full Ca/Mn A/A′ order and only 4.0(1)% Mn/Re B/B′-antisite disorder).[8] A ferrimagnetic transition at T_C = 120 K was observed in magnetisation measurements and magnetic hysteresis at 3 K revealed a saturated magnetisation of $m_s = 3.4\mu_B$, and a notable coercive field of 1.6 T reflecting strong anisotropy from spin–orbit coupling in $5d^1$ Re^{6+}. Neutron diffraction revealed two spin ordering transitions, an antiferromagnetic ordering of B-site Mn/Re spins in the *ab*-plane at 120 K and ferrimagnetic order of A-site Mn spins parallel to *c* at 100 K. This complex spin ordering is unusual in DDPv's, where ferrimagnetic order of all spins parallel or antiparallel to the *c*-axis is most common.[5] Hence, the present La^{3+} doping study has been performed to investigate whether the DDPv structure is robust to doping, and if so how the magnetic properties change.

$La_xCa_{1-x}MnMnReO_6$ compositions with x = 0.25, 0.50, and 0.75 were treated under high pressure-high temperature

[a] Centre for Science at Extreme Conditions (CSEC) and School of Chemistry, University of Edinburgh, Edinburgh EH9 3FD, UK. E-mail: j.p.attfield@ed.ac.uk
[b] Institut Laue-Langevin, 38042 Grenoble, France

(HPHT) conditions using a Walker type multianvil apparatus. $CaMnO_3$, $LaMnO_3$, MnO and ReO_2 reactants were mixed in stoichiometric ratios, packed in a Pt capsule, compressed to 10 GPa pressure, and heated at 1000 °C for 30 minutes before quenching to room temperature and slowly depressurising to ambient conditions. X-ray powder diffraction (XPD) from a Bruker D2 diffractometer (CuKα radiation, $5^\circ \leq 2\theta \leq 70^\circ$) was used for sample characterisation. A Quantum Design PPMS was used to collect variable temperature and field magnetisation data. Neutron powder diffraction (NPD) data from composite samples of the three compositions (made by combining 3–4 high pressure products) were collected on the D20 beamline at the ILL facility at temperatures 1–2, 50, 100, 150, 200, and 250 K using a wavelength of 2.40 Å for crystal and magnetic structure refinement. Fullprof software was used to fit diffraction data.[15]

XPD data in Fig. 1a show that $La_xCa_{1-x}MnMnReO_6$ samples for $x = 0.25$ and 0.50 are near phase-pure DDPv's and with small amounts of MnO (4.8 and 7.2% respectively), but $x = 0.75$ has further secondary phase contributions showing that this composition lies above the limit for La substitution under the HPHT synthesis conditions used. Fits to these data (shown in SI) of a $P4_2/n$ DDPv model (Fig. 1b) give the cell parameters shown in Table 1.

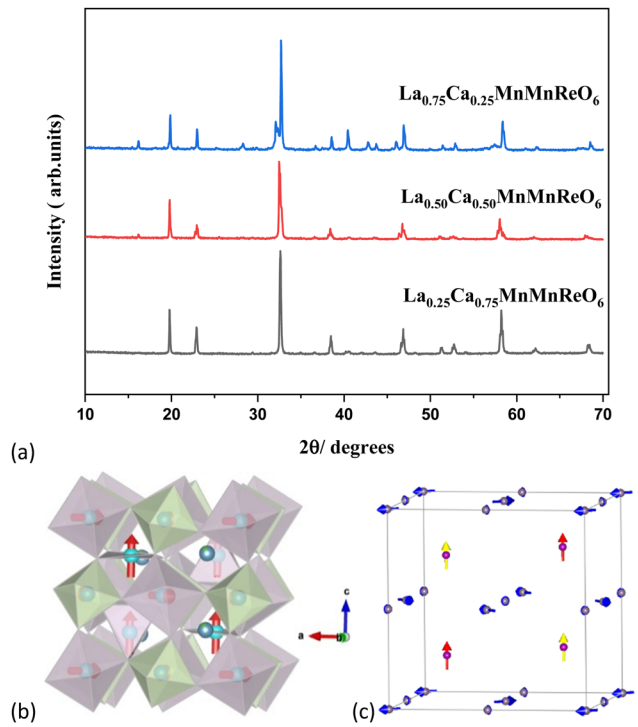

Fig. 1 (a) XPD patterns for HPHT-synthesised $La_xCa_{1-x}MnMnReO_6$ samples with nominal compositions as shown. (b) Tetragonal $P4_2/n$ DDPv $La_xCa_{1-x}MnMnReO_6$ crystal structure model. La/Ca and Mn are ordered in A-site columns with Mn further ordered into tetrahedral and square planar environments, while MnO_6 and ReO_6 octahedra have rocksalt-type order at the B-sites. Magnetic moments are also shown in red. (c) Magnetic structure model. A-site Mn moments (red and yellow) are ferromagnetically ordered parallel to the *c*-axis, while B-site Mn and Re spins (large and small blue arrows) are antiferromagnetically ordered and rotated by 90° relative to their neighbours in the in the *ab*-plane.

Table 1 Summary of structural and magnetic parameters for $La_xCa_{1-x}MnMnReO_6$ DDPvs. $x = 0$ values are from ref. 8, and others are from this work. Results from top to bottom are; cell parameters from fits to 300 K XPD data; refined La/Ca and Mn(Re) (= B/B′ inversion) site occupancies from 250 K NPD fits; Curie temperature T_C, coercive field H_c at 2 K, and saturated magnetisation per formula unit (f.u.) m_s at 2 K and 9 T from magnetisation measurements; and refined Mn moment (equivalent to the net saturated moment per f.u.) from 2 K NPD fits

x	0	0.25	0.50	0.75
Cell parameters				
a/Å	7.7080(2)	7.7680(5)	7.793(1)	7.738(1)
c/Å	7.7730(3)	7.7442(9)	7.763(3)	7.726(2)
V/Å^3	459.44(2)	467.29(7)	471.5(2)	462.6(1)
Site occupancies				
A-La(Ca)/%	0	14(2)	48(2)	75
B-Mn(Re)/%	4.0(1)	4.0(6)	0	14(1)
Magnetic parameters				
T_c/K	120	145	185	185
H_c/T	1.38	0.36	0.13	0.14
m_s/μ_B f.u^{-1}	3.4	2.0	2.0	1.3
mMn/μ_B	2.70(6)	1.09(8)	0.83(9)	0.9(2)

NPD data were collected from the three $La_xCa_{1-x}MnMnReO_6$ samples at temperatures between 1.4 and 250 K for structure refinement and to discover any low temperature spin ordering. However, substantial amounts of unidentified impurities were present for $x = 0.75$ and this prevented accurate refinement of atomic coordinates and the La/Ca occupancy was fixed at the nominal value. The high scattering length (b) contrasts between the metals (La/Ca/Mn/Re have respective b = 8.24/4.70/−3.73/9.2 fm) enable accurate cation site occupancies to be determined. Refined site occupancies in Table 1 show that the $x = 0.25$ sample is apparently La-deficient, but the refined value for $x = 0.50$ is very close to the ideal value. A small (4%) disorder of B-site Mn/Re cations is found in $x = 0$ and 0.25 samples, but for $x = 0.50$ there was no refinable inversion.

$CaMnMnReO_6$ was previously found to have an unusual low temperature spin order (Fig. 1c) where A-site Mn moments are ferromagnetically ordered parallel to the *c*-axis, while B-site Mn and Re spins are antiferromagnetically ordered in the *ab*-plane. This is characterised by an intense (001) magnetic diffraction peak, which is not observed for the simple ferrimagnetic order observed in the majority of DDPvs where all spins are parallel to *c*. The same peak is observed for the three $La_xCa_{1-x}MnMnReO_6$ samples, although with lower intensity, demonstrating that the same spin ordering is present but with smaller ordered moments. This model was fitted to the low temperature NPD data (Fig. 2b) with constraints that the magnitude of all Mn moments are the same, and with the Re moment having 20% of this value (based on ideal Mn^{2+} $S = 5/2$ and Re^{6+} $S = \frac{1}{2}$ spin-only values). As data were collected in 50 K intervals and magnetic contributions from the $La_xCa_{1-x}MnMnReO_6$ phases were too weak to be fitted reliably above 100 K, it was not possible to determine A or B-site spin ordering transition temperatures, and whether these coincide or not, by NPD. However, the observed magnetic diffraction is

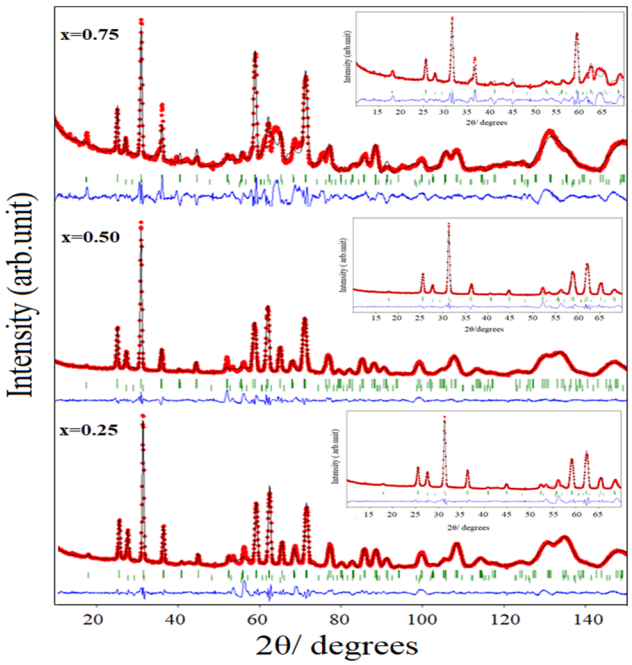

Fig. 2 Rietveld fits of crystal and magnetic structure to NPD data for $La_xCa_{1-x}MnMnReO_6$ samples at 2 K. Insets of the low angle region show the DDPv (001) magnetic peak at $2\theta = 18°$ (this has an overlapping impurity peak for $x = 0.75$), and also a broad magnetic peak from MnO at 27°. Bragg markers from top to bottom are for $La_xCa_{1-x}MnMnReO_6$ (nuclear and magnetic) and MnO (magnetic and nuclear) phases.

consistent with bulk T_C values of 120–185 K from magnetisation measurements as described below. Refined Mn moments at 2 K for the $La_xCa_{1-x}MnMnReO_6$ samples are shown in Table 1 and plots showing the thermal evolution of the moments are in SI.

Magnetic susceptibility and magnetisation-field plots for the three $La_xCa_{1-x}MnMnReO_6$ samples are shown in Fig. 3. All three show a Curie transition that increases to higher temperature with La content, but the $x = 0.75$ sample shows a pronounced second transition near 100 K which is mostly likely due to a secondary phase. All samples show magnetic hysteresis at 2 K and the extracted saturated magnetisations M_s and coercive fields H_c are displayed in Table 1. Comparison against the reported loop for $CaMnMnReO_6$ in Fig. 3g reveals that La doping leads to a decrease in M_s and a dramatic fall in H_c.

The results above demonstrate that La doping in the double double perovskite system $La_xCa_{1-x}MnMnReO_6$ has been achieved for $x = 0.25$ and 0.50. This is evidenced by the increase of unit cell volume with x in Table 1, consistent with La^{3+} being larger than Ca^{2+}, and also with electron-doping of the lattice (reduction of Re^{6+} to slightly larger Re^{5+}). However, the sample with nominal composition $x = 0.75$ is inhomogenous showing that the solid solution limit under the synthesis conditions used (10 GPa and 1000 °C) lies between $x = 0.50$ and 0.75. Structure refinements against X-ray and neutron diffraction data confirm that the $P4_2/n$ $AA'BB'O_6$ double double perovskite (DDPv) superstructure is maintained throughout. It is particularly notable that the $La_xCa_{1-x}MnMnReO_6$ composition with maximum La/Ca-site disorder ($x = 0.50$) has been synthesised as

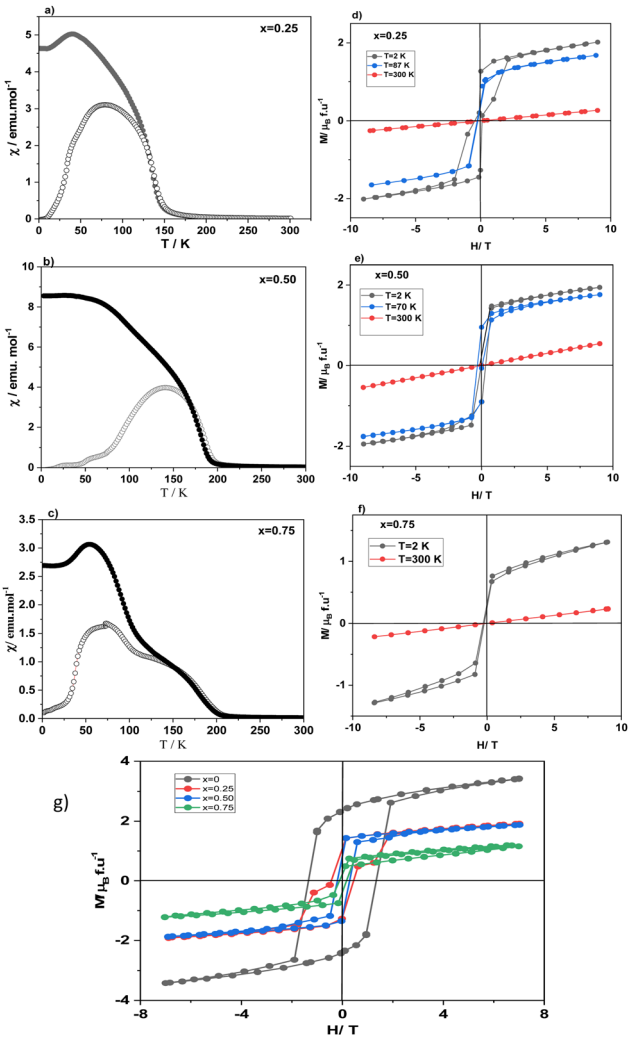

Fig. 3 Magnetisation data for the $La_xCa_{1-x}MnMnReO_6$ samples (x = 0.25, 0.50 and 0.75). (a)–(c) Magnetic susceptibilities (open/closed symbols = zero field cooled/field cooled data) in a 0.1 T field. (d)–(f) Magnetisation (M)–field (H) hysteresis loops at several temperatures. (g) Comparison of 2 K M–H loops for $x = 0$ (from ref. 8) and the above three samples showing data in the range $H = \pm 7$ T to demonstrate the 'wasp-waist' feature for x = 0.25 and 0.50.

a solid solution without loss of A/A′ or B/B′ cation-site orders, demonstrating that the DDPv structure type can be robust to chemical tuning through aliovalent doping. BVS's calculated from the 250 K NPD refinements (shown in SI) confirm that all Mn cations remain in the +2 state for the $x = 0$ to 0.5 materials, while the Re valence is between 5 and 6, although no systematic reduction is seen for Re, probably because Re–O distances change little in these high oxidation states. X-ray absorption spectroscopy or other valence sensitive techniques would be needed to measure changes in oxidation state directly.

There is also clear evidence for systematic tuning of magnetic properties through the electron-doping effect in the $La_xCa_{1-x}MnMnReO_6$ solid solutions. The Curie temperature T_C increases 120 → 185 K for $x = 0$ → 0.50, most likely because the increasing number of unpaired Re d-electrons (= 1 + x)

strengthens superexchange pathways within the Mn/Re B-site framework. NPD shows that the unusual combined ferromagnetic A′ = Mn and antiferromagnetic B/B′ = Mn/Re spin orders of $CaMnMnReO_6$ are maintained in $La_xCa_{1-x}MnMnReO_6$ solid solutions. However, the magnitude of the saturated ferrimagnetic magnetisation, and of ordered Mn^{2+} moments measured by NPD, both decrease with x due to the structural (La^{3+}/Ca^{2+}) and electronic (Re^{5+}/Re^{6+}) disorder effects of doping. $CaMnMnReO_6$ was previously shown to have separate spin ordering transitions, of B-site Mn/Re spins at 120 K and of A-site Mn spins at 100 K, and it is not clear whether this is maintained in the $x > 0$ samples or if disorder leads to merging of the two transitions. Further NPD studies will be needed to resolve this.

The most remarkable tuning effect in the $La_xCa_{1-x}MnMnReO_6$ system is of the low temperature magnetic coercivity, which decreases from magnetically-hard (H_c = 1.4 T) at x = 0 to quite soft ($H_c \approx$ 0.1 T) behaviour for x = 0.50. H_c is a measure of magnetic anisotropy which can have both structural and electronic contributions. The electronic aspect is dominant here as $5d^1$ Re^{6+} gives strong anisotropy from spin–orbit coupling whereas $5d^2$ Re^{5+} is less electronically anisotropic in a comparable DDPv $CaMnFe^{3+}Re^{5+}O_6$ which has H_c = 0.04 T.[8] A similar decrease in coercive field is seen in double perovskites; $Ca_2Mn^{2+}Re^{6+}O_6$ has H_c = 4 T,[16] whereas $Ca_2Fe^{3+}Re^{5+}O_6$ has H_c = 1 T at base temperature,[17] although here a monoclinic distortion gives a larger structural contribution to the magnetic anisotropy. Hysteresis loops in Fig. 3g give insights into how coercivity falls as Re^{6+} is doped towards Re^{5+}. The 'wasp-waist' shape of the 2 K hysteresis loop for the x = 0.25 sample, and to a lesser extent x = 0.50, shows that the system evolves *via* a mixture of decreasing large-coercivity and increasing small-coercivity components. This effect could be due to inhomogeneity in the chemical doping, although there is no evidence for this in the diffraction data, so a more likely explanation is that the disorder created by La^{3+}/Ca^{2+} doping leads to a range of magnetic domain sizes, with smaller, less anisotropic domains having smaller H_c than larger or more anisotropic domains.

In conclusion, this study demonstrates that a member of the $P4_2/n$ AA′BB′O6 double double perovskite family of perovskites can be systematically doped by a standard substitution mechanism. Remarkably, full A/A′ and B/B′ cation ordering is preserved in the $La_xCa_{1-x}MnMnReO_6$ system up to a limit between x = 0.5 and 0.75, but with continuous La^{3+}/Ca^{2+} substitution at the A-site, charge compensated by reduction of Re^{6+} to Re^{5+}. Tuning of magnetic properties is demonstrated as the ferrimagnetic Curie temperature increases with x while the magnetisation and in particular the coercivity fall off. Around 20 isostructural DDPv's have been discovered through HPHT synthesis in recent years, each of which could also be chemically doped through aliovalent substitution or other mechanisms, so there are clearly many possibilities to discover and tune electronic and magnetic properties within this emerging family of materials.

Conceptualisation by AA, SDI, KJ and JPA. Investigation and formal analysis performed by AA, SDI, KJ and CR. Original draft written by AA and JPA, with reviewing and editing by all authors.

We thank EPSRC for support and STFC for provision of beamtime at the ILL.

Conflicts of interest

There are no conflicts to declare.

Data availability

Data that support the findings of this study are available at: **https://doi.org/10.7488/ds/7968**. ILL data are at: **https://doi.org/10.5291/ILL-DATA.5-31-3020**.

Supporting figures and tables, cif files from 2 K NPD refinments. See DOI: **https://doi.org/10.1039/d5cc03601a**

Notes and references

1 X. Xu, Y. Zhong and Z. Shao, *Trends Chem.*, 2019, **1**, 410–424.
2 D. Sánchez, J. A. Alonso, M. García-Hernández, M. J. M. García-Hernández, M. T. Casais and J. L. Martinez, *J. Mater. Chem.*, 2003, **13**, 1771–1777.
3 G. King and P. M. Woodward, *J. Mater. Chem.*, 2010, **20**, 5785–5796.
4 G. King and S. Garcia-Martin, *Inorg. Chem.*, 2019, **58**, 14058.
5 E. Solana-Madruga and A. M. Arévalo-López, *J. Solid State Chem.*, 2022, **315**, 123470.
6 E. Solana-Madruga, A. M. Arévalo-López, A. J. Dos Santos-Garca, E. Urones-Garrote, D. Avila-Brande, R. Saez-Puche and J. P. Attfield, *Angew. Chem., Int. Ed.*, 2016, **55**, 9340–9344.
7 K. Ji, Y. Yuan, G. T. Moyo, C. Ritter and J. P. Attfield, *J. Solid State Chem.*, 2022, **313**, 123329.
8 G. M. McNally, A. M. Arevalo-López, P. Kearins, F. Orlandi, P. Manuel and J. P. Attfield, *Chem. Mater.*, 2017, **29**, 8870–8874.
9 E. Solana-Madruga, Y. Sun, A. M. Arévalo-López and J. P. Attfield, *Chem. Commun.*, 2019, **55**, 2605–2608.
10 G. McNally, A. Arévalo-López, F. Guillou, P. Manuel and J. P. Attfield, *Phys. Rev. Mater.*, 2020, **4**, 064408.
11 E. Solana-Madruga, P. S. Kearins, C. Ritter, A. M. Arévalo-López and J. P. Attfield, *Angew. Chem., Int. Ed.*, 2022, **61**, e202209497.
12 K. Ji, J. R. Bedward, Q. Li, P. Manuel, C. Ritter and J. P. Attfield, *Chem. Commun.*, 2023, **59**, 6371–6374.
13 A. M. Arévalo-López, G. M. McNally and J. P. Attfield, *Angew. Chem., Int. Ed.*, 2015, **54**, 12074–12077.
14 K. Ji, K. N. Alharbi, E. Solana-Madruga, G. T. Moyo, C. Ritter and J. P. Attfield, *Angew. Chem., Int. Ed.*, 2021, **60**, 22248–22252.
15 J. Rodriguez-Carvajal, *Physica B*, 1993, **192**, 55.
16 A. S. Cavichini, M. T. Orlando, J. B. Depianti, J. L. Passamai, Jr., F. Damay, F. Porcher and E. Granado, *Phys. Rev. B*, 2018, **97**, 054431.
17 J. M. Michalik, J. M. De Teresa, J. Blasco, P. A. Algarabel, M. R. Ibarra, C. Kapusta and U. Zeitler, *J. Phys.: Condens. Matter*, 2007, **19**, 506206.

